RSC Advances

PAPER

View Article Online
View Journal | View Issue

# Cascade OFF–ON–OFF fluorescent probe: dual detection of trivalent ions and phosphate ions†

Cite this: *RSC Adv.*, 2014, **4**, 29479

Xuejuan Wan,‡*[ab] Tianqi Liu,‡[a] Haiyang Liu,[b] Liqiang Gu[b] and Youwei Yao*[b]

Received 13th April 2014
Accepted 16th June 2014

DOI: 10.1039/c4ra03339f

www.rsc.org/advances

A new rhodamine B-based fluorescent probe was developed for the selective cascade signaling of trivalent cations ($Fe^{3+}$, $Al^{3+}$, $Cr^{3+}$) and phosphate anion ($PO_4^{3-}$). Non-fluorescent rhodamine derivatives can selectively detect trivalent cations over some other metal ions in $CH_3CN$–Tris buffer (1/1, v/v, pH 7.0) solutions, leading to prominent fluorescence OFF–ON switching. The obtained probe–cation complex can subsequently serve as a sensitive and selective chemosensor for $PO_4^{3-}$, exhibiting complete signal quenching (fluorescence ON–OFF switching).



## Introduction

The fluorogenic sensing of different metal ions has become particularly attractive because of its simplicity, high sensitivity, and instantaneous response.[1–6] Among them, triple-charged metal cation detection is of significant importance because of its crucial influence in a wide range of environmental and human health areas.[7–17] For example, $Fe^{3+}$ ion is an essential element in the human body and acts as a cofactor in several enzymatic reactions;[18–20] whereas the widely existing $Al^{3+}$ ion in the environment is considered to be toxic in biological activities, and responsible for the Parkinson's disease;[21,22] for $Cr^{3+}$, which is also an effective nutrient for the human body, a deviation of its concentration from normal levels can increase the risk of diabetes and cardiovascular diseases.[40] Simultaneously, the detection of anions through fluorescence emission readouts has also attracted significant attention considering the recognized biological roles played by anions.[23] However, it is difficult to recognize anions in water or in a water mixture media compared with most of the metal cations because anions usually experience competition from the solvent for sensor binding sites.[24] Nevertheless, a metal complex may resolve this problem *via* a simple displacement approach, causing a signal change in the UV-vis or fluorescence spectrum.[25–28] Phosphate anions ($PO_4^{3-}$), both inorganic and organic, have a unique position in nature because they participate in almost all the metabolic processes.[29,30] Moreover, phosphorylated biomolecules play an important role in signal transduction for various biological processes. Human serum contains 0.80–1.45 mM phosphate but higher phosphate levels are directly connected to cardiovascular disease and acute renal failure.[31]

Up till now, even though a large number of fluorescence chemosensors for divalent metal ions and phosphate anions have been reported in the literature, relatively few studies have been devoted to the development of fluorescence sensors which are sensitive to trivalent ions[41–43] and phosphate ions.[39] In view of achieving a rapid qualitative analysis of the pollutants, it is highly desirable to design a probe which is capable of simultaneous discrimination of trivalent ions and phosphate ions from other ions.

Herein, we report a simple cascade "OFF–ON–OFF" fluorescent chemosensor for trivalent and phosphate ions based on the equilibrium between spirolactam (non-fluorescent) to the ring-open amide (fluorescent) form of rhodamine chromophore.[4,9,32] In general, the chemosensor showed a specific selectivity toward trivalent ions over other common metal ions, leading to prominent fluorescence OFF–ON switching. The resultant sensor–cation complex could selectively recognize $PO_4^{3-}$ over other anions, exhibiting complete ON–OFF signal quenching.

## Experimental

### Materials and methods

Rhodamine B was obtained from Aladdin. Phthalic anhydride and hydrazine hydrate were purchased from Sinopharm Chemical Reagent. The solution of metal ions was prepared from their chloride salts of analytical grade. The solvents were used as-received without further purification. Deionized water was used throughout the experiment.

UV-vis spectra were recorded using a SCINCO S-4100. A HORIBA Jobin Yvon SPEX spectrofluorimeter was used for fluorescence measurements. The excitation wavelength was 520 nm and the spectra were recorded in the range of 540–700 nm. Both $^1H$ NMR (400 MHz) and $^{13}C$ NMR spectra (100 MHz) of

[a]*Shenzhen Key Laboratory of Special Functional Materials, College of Materials Science and Engineering, Shenzhen University, Shenzhen 518060, PR China. E-mail: wanxj@szu.edu.cn*

[b]*Advanced Materials Institute, Graduate School at Shenzhen, Tsinghua University, Shenzhen 518055, PR China. E-mail: yaoyw@sz.tsinghua.edu.cn*

† Electronic supplementary information (ESI) available. See DOI: 10.1039/c4ra03339f

‡ These authors contributed equally to the work.

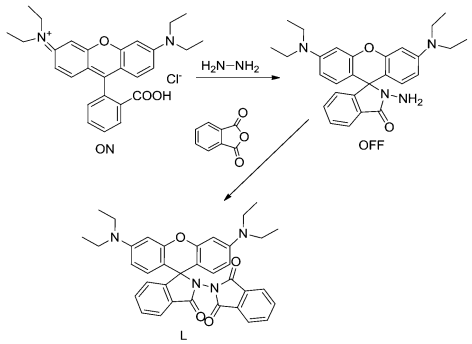


Scheme 1 Schematic illustration of the synthesis of an RhB-based fluorescence probe L.

the compounds were recorded on a Brurker Dpx spectrometer in $CDCl_3$ with tetramethylsilane as the internal standard. The high-resolution mass spectra were recorded on a Bruker APEX IV.

### Synthetic methodology

Compound L was synthesized in two steps, as shown in Scheme 1. Rhodamine B hydrazide was first synthesized following literature procedures.[32] Phthalic anhydride (100 mg, 0.67 mmol) was added to a solution of rhodamine B hydrazide (300 mg, 0.66 mmol), which was dissolved in 40 mL anhydrous toluene. The reaction mixture was heated under microwave irradiation for 30 minutes and allowed to cool to room temperature. After that, the solvent was removed under reduced pressure, and the crude product was purified with a silica gel column using a mixture of petroleum ether and ethyl acetate (2 : 1, v/v) as an eluent to afford a yellow solid in a 30% yield. $^1$H NMR (Fig. S1†) (400 MHz, $CDCl_3$) $\delta$ 8.02 (d, $J$ = 7.4 Hz, 1H), 7.75–7.65 (m, 4H), 7.62 (t, $J$ = 7.2 Hz, 1H), 7.56 (t, $J$ = 7.2 Hz, 1H), 7.25 (d, $J$ = 7.5 Hz, 1H), 6.83 (d, $J$ = 8.9 Hz, 2H), 6.40 (d, $J$ = 6.4 Hz, 2H), 6.26 (d, $J$ = 2.3 Hz, 2H), 3.42–3.26 (m, 8H), 1.16 (t, $J$ = 7.0 Hz, 12H). $^{13}$C NMR (Fig. S2†) (100 MHz, $CDCl_3$) $\delta$ (ppm) 164.07, 153.68, 153.06, 149.47, 148.82, 133.97, 133.40, 130.88, 130.09, 128.32, 124.45, 123.64, 123.40, 107.52, 104.23, 97.01, 73.37, 44.18, 12.47. HRMS (ESI) (Fig. S3†): calcd for $C_{36}H_{35}N_4O_4$ $[M + H^+]^+$: 587.2658; found: 587.2652.

## Results and discussion

The equilibrium between the non-fluorescent spirolactam form and the fluorescent ring-open amide form of rhodamine derivatives has been proven to be an efficient platform for the construction of fluorescent sensors for numerous heavy metal cations (such as $Hg^{2+}$, $Pb^{2+}$ and $Cu^{2+}$) due to its large absorption coefficient and high fluorescence quantum yield.[33–35] In the current work, this typical ion-recognition mechanism was utilized for the successive detection of trivalent ions and then phosphate ions *via* fluorescence OFF–ON–OFF switching.

### Fluorescence OFF–ON sensing for $Fe^{3+}$, $Al^{3+}$ and $Cr^{3+}$

The detection selectivity of probe L (10 μM) toward $Fe^{3+}$ ions was investigated by monitoring the fluorescence changes upon the addition of 8 equiv. chloride salts of a wide range of cations in $CH_3CN$–Tris-buffer (1/1, v/v, pH 7.0) media, including $Na^+$, $K^+$, $Mg^{2+}$, $Cu^{2+}$, $Hg^{2+}$, $Cd^{2+}$, $Fe^{2+}$, $Pb^{2+}$, $Zn^{2+}$, $Mn^{2+}$, $Ca^{2+}$, $Fe^{3+}$, $Al^{3+}$ and $Cr^{3+}$. The fluorescence emission spectra of L were measured in 1.0 cm quartz cells, and the excitation and emission slits were set to 2.0 and 2.0 nm, respectively. As shown in Fig. 1, the sensor itself was almost non-fluorescent due to its ring-closed spirolactam structure. After the addition of $Fe^{3+}$, probe L exhibited a color change from colorless to pink as well as a bright red fluorescence. A strong emission band centered at 586 nm was observed with an extreme fluorescence enhancement compared to the metal-free L. This result indicated that the probe L exhibited a high selectivity toward $Fe^{3+}$ over the monovalent and divalent cations in $CH_3CN$–Tris-buffer (1/1, v/v, pH 7.0) media.

To further explore the selectivity of the sensor, competitive ions were first added to the detection solution, and then $Fe^{3+}$ ions were added after 20 minutes. As shown in Fig. 2, most of the detection systems exhibited minimum interference in the detection of $Fe^{3+}$; $Al^{3+}$ and $Cr^{3+}$ (80 μM each) also did not induce any obvious interference in the fluorescence sensing of $Fe^{3+}$, indicating that L has a relatively higher binding affinity to $Fe^{3+}$ than $Al^{3+}$ and $Cr^{3+}$. In addition, the association constants were $6.13 \times 10^4$ for L–$Fe^{3+}$, $3.14 \times 10^4$ for L–$Al^{3+}$ and $2.26 \times 10^4$ for L–$Cr^{3+}$, according to the reported work,[44,45] respectively. A similar study was carried out with $Al^{3+}$ and $Cr^{3+}$, and there were no obvious interferences in the presence of $Na^+$, $K^+$, $Mg^{2+}$, $Cu^{2+}$, $Hg^{2+}$, $Cd^{2+}$, $Fe^{2+}$, $Pb^{2+}$, $Zn^{2+}$, $Mn^{2+}$ and $Ca^{2+}$.

The sensing property of L was investigated in detail utilizing the $Fe^{3+}$ cation. Fig. 3 displays the absorption spectrum changes of L upon $Fe^{3+}$ addition. Sensor L exhibited almost no absorption peak in the visible wavelength due to the spirolactam form of molecule L. However, a new band centered at about 562 nm emerged upon the gradual addition of $Fe^{3+}$, indicating the sensor L–$Fe^{3+}$ complex formation and $Fe^{3+}$-induced spirolactam ring-opening processes. Moreover, the titration solution displayed a characteristic color change of rhodamine derivatives from colorless to pink, indicating that probe L could serve as a "naked-eye" indicator for $Fe^{3+}$ in $CH_3CN$–Tris-buffer (1/1, v/v) media. With increasing amounts of $Fe^{3+}$, the absorbance increased proportionally and levelled off when the

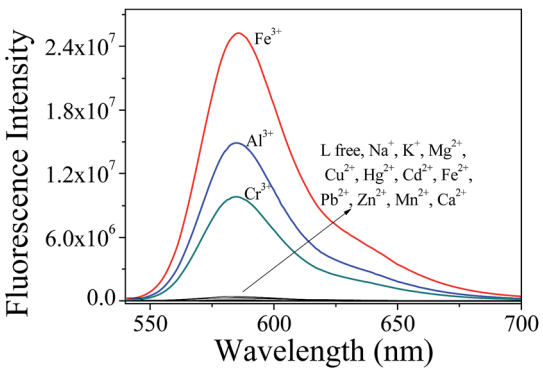


Fig. 1 Fluorescence spectra of L (10 μM) in the presence of various metal ions (80 μM each) in $CH_3CN$–Tris-buffer (1/1, v/v, pH 7.0), $\lambda_{ex}$ = 520 nm.

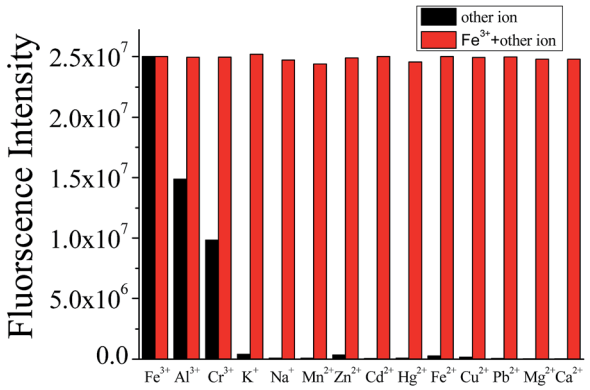


Fig. 2 Change in fluorescence intensity of L (10 μM) in various mixtures of metal ions (the concentration of $Fe^{3+}$ and other metal ions were all 80 μM).

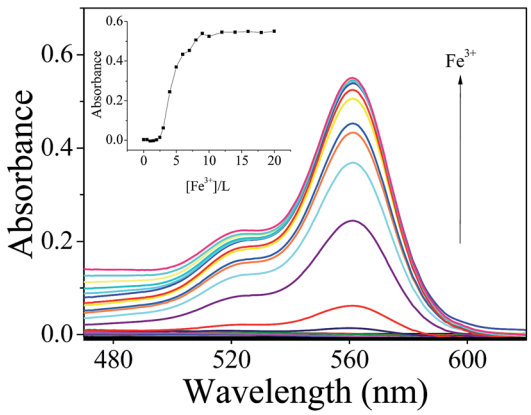


Fig. 3 UV-vis spectra and (inset) absorbance changes (564 nm) recorded for L (25 μM) in $CH_3CN$–Tris (1/1, v/v) with various amounts of $Fe^{3+}$ ions.

concentration of $Fe^{3+}$ reached 250 μM. When UV-vis titration measurements were carried out with $Al^{3+}$ (Fig. S4†) and $Cr^{3+}$ (Fig. S5†), similar changes were found to those of $Fe^{3+}$, *i.e.*, absorbance increased at first and then levelled off.

Appropriate pH conditions for the successful operation of the fluorescence sensing were evaluated. Without the addition of the $Fe^{3+}$ ion, the ring opening of the RhB-based sensor L occurred under acidic conditions (pH < 5.0) due to protonation, while no fluorescence change was observed with pH values over 5 (Fig. 4). The gradual addition of $Fe^{3+}$, however, led to an obvious fluorescence enhancement over a wide pH range from 5.0 to 8.0, which was attributed to the similar opening of the spirolactam structure.[36] Because the most remarkable $Fe^{3+}$-induced OFF–ON fluorescence changes occurred under the physiological pH window, all the fluorescence measurements were conducted at pH 7.0. Similar phenomenon can also be observed in the fluorescence sensing of $Al^{3+}$ and $Cr^{3+}$, as shown in Fig. S6.†

The relative affinities of $Fe^{3+}$ toward sensor L were evaluated from fluorescence spectroscopic titration experiments in $CH_3CN$–Tris-buffer (1/1, v/v) medium, as shown in Fig. 5. The

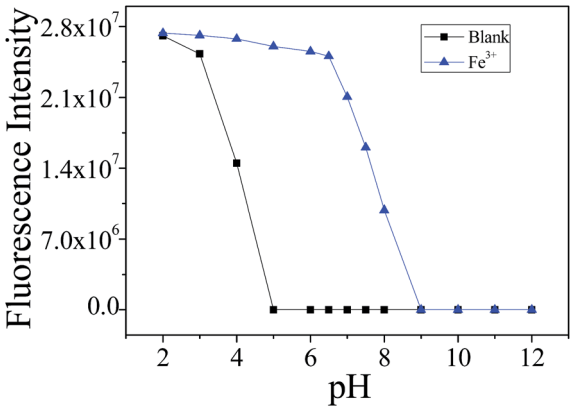


Fig. 4 Fluorescence intensities recorded for L (10 μM, $CH_3CN$–$H_2O$ 1 : 1, v/v) at various pH values in the (a) absence and (b) presence of 8 equiv. $Fe^{3+}$ ($\lambda_{ex}$ = 520 nm, $\lambda_{em}$ = 586 nm).

concentration of L was maintained at 10 μM, while the concentration of $Fe^{3+}$ was varied between 0 and 250 μM. The fluorescence spectra were recorded at an excitation wavelength of 520 nm and emission wavelength of 540–700 nm. For free L, no obvious characteristic emission of rhodamine derivatives was observed. With increasing concentrations of $Fe^{3+}$, the fluorometric titration reaction curve showed a steady and smooth enhancement, which was used as the basis of $Fe^{3+}$-sensing. The recognition interaction was completed immediately after the addition of $Fe^{3+}$, *i.e.*, within 1 min. When the concentration of $Fe^{3+}$ was greater than 200 μM, the fluorescence intensity did not increase any further and a plateau was reached. The inset in Fig. 5 shows the dependence of fluorescence intensity at 586 nm on $Fe^{3+}$ concentration. Plotting fluorescence intensity *versus* $Fe^{3+}$ concentration (1–4 equiv.) afforded a good linear relationship ($R$ = 0.9844) (Fig. S7†). The detection limit of $Fe^{3+}$ was calculated from the equation DL = $(3S_{b1} - I)/S$ instead of DL = $3S_{b1}/S$ (ref. 37 and 38) because the intercept is not negligible, where $S_{b1}$ is the standard deviation of the blank solution, $I$ is the intercept and $S$ is the slope of the

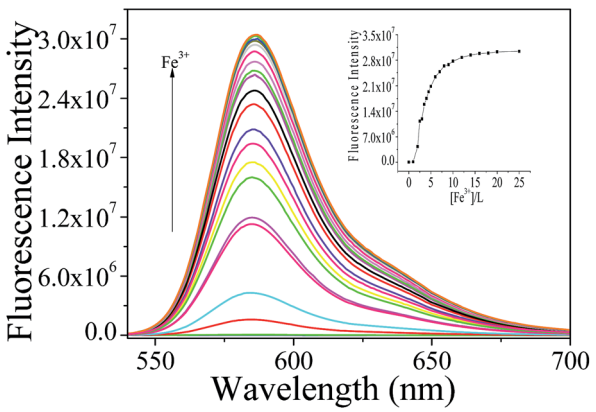


Fig. 5 Fluorescence titrations of L (10 μM) with $Fe^{3+}$ ions in $CH_3CN$–Tris (1/1, v/v, pH 7.0). Inset: fluorescence emission intensity changes with increasing $Fe^{3+}$ ions ($\lambda_{ex}$ = 520 nm, $\lambda_{em}$ = 586 nm).

calibration curve. The detection limit of L for $Fe^{3+}$ was 1.10 × $10^{-5}$ M. And the detection limits of L were 3.20 × $10^{-7}$ M (Fig. S8 and S9†) for $Al^{3+}$ and 2.55 × $10^{-5}$ M for $Cr^{3+}$ (Fig S10 and S11†).

To determine the interaction stoichiometry between sensor L and $Fe^{3+}$, Job's method was employed using an absorbance intensity at 562 nm as a function of molar fraction of L because the total concentration of L and $Fe^{3+}$ ion was located at 50 μM. The maximum absorbance was observed when the molar fraction of L reached 0.50 (Fig. 6), which was indicative of a 1 : 1 stoichiometry complexation between L and $Fe^{3+}$. This result was further confirmed by high-resolution mass spectrum (HR-MS Fig. S12†), in which the peak at *m*/*z* 786.0831 (calcd = 786.0811) corresponding to $[L + Fe^{3+} + 2H^+ + 4Cl^-]^+$ was clearly observed when 5 equiv. of $FeCl_3$ was added to probe L. Similarly, the stoichiometric ratios were 1 : 1 for $Al^{3+}$ (Fig. S13†) and $Cr^{3+}$ (Fig. S14†). As inferred by FTIR (Fig. S15†), the structure of the L–$M^{3+}$ complex was proposed, as shown in Fig. S16.† When probe L was treated with $Fe^{3+}$, the characteristic amide carbonyl absorption peak at 1631 $cm^{-1}$ shifted to 1608 $cm^{-1}$, indicating that the amide carbonyl O of rhodamine B unit was actually involved in the recognition of $Fe^{3+}$, which also agreed with the previously reported work.[46,47]

### Fluorescence ON–OFF sensing for $PO_4^{3-}$

Interestingly, when the L–$Fe^{3+}$ complex was treated with a sodium salt of $PO_4^{3-}$, the color of the solution changed from pink to colorless, and the emission was completely quenched within 1 min (Fig. 7a), while other anions, such as $Cl^-$, $Br^-$, $I^-$, $SO_4^{2-}$, $SO_3^{2-}$, $HPO_4^{2-}$, $H_2PO_4^-$, $NO_3^-$, did not show any interference to the detection. This observation suggested that the probe L could not only act as a sensor for $Fe^{3+}$ but also for $PO_4^{3-}$ in a successive manner. Once the $Fe^{3+}$ ion interacted with the sensor L, the spirolactum ring was opened, yielding a high fluorescence emission. However, when treated with the $PO_4^{3-}$ anion, the metal ion was abstracted and the spirolactum ring closed, leading to the absence of fluorescence. The $PO_4^{3-}$ anion-sensing capability of the obtained complex was further investigated in detail with fluorescence titration analysis (Fig. 7b). The titration curve showed an excellent linear decrease, and about 1.0 equiv. of $PO_4^{3-}$ (compared with $Fe^{3+}$) was required to obtain absolute fluorescence quenching. The detection limit was calculated to be 0.20 μM (Fig. S17†) according to the fluorescence titration curve, which reveals a high sensitivity for the analysis of phosphate ion using the L-$Fe^{3+}$ complex. The $Al^{3+}$ complex can also serve as a sensor for $PO_4^{3-}$ *via* a simple displacement approach because of the strong affinity of $PO_4^{3-}$ to $Al^{3+}$. Moreover, the cascade fluorescence OFF–ON–OFF response can be observed with the alternate addition of $Fe^{3+}$ cation and $PO_4^{3-}$ anion into the detection solution (Fig. S18†), suggesting that the obtained fluorescence probe L can respond to both the cation and anion even when they co-exist in the solution. EDTA was further used to investigate the reversibility of the $Fe^{3+}$ sensing process (Fig. S19†). The results indicate that EDTA could also cause an "ON–OFF" response of the L–$Fe^{3+}$ complex *via* chelation. After the addition of excess $Fe^{3+}$ to the detection solution, the recovered fluorescence emission can be clearly observed, suggesting that the probe exhibits good detection reversibility.

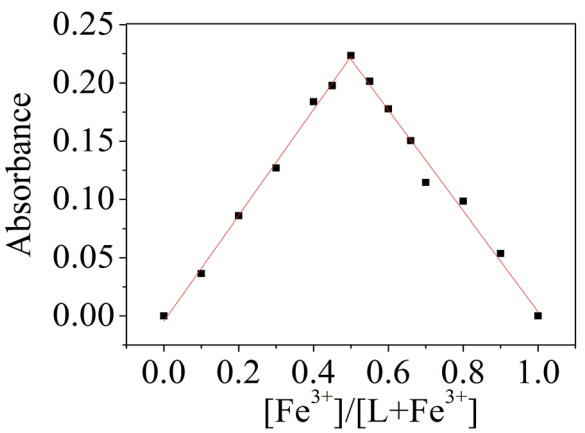


Fig. 6 Job's plot obtained for the determination of binding stoichiometry between L and $Fe^{3+}$ in $CH_3CN$–Tris (1/1, v/v). The total concentration of L and $Fe^{3+}$ was maintained at 50 μM. Absorbance was measured at 564 nm.

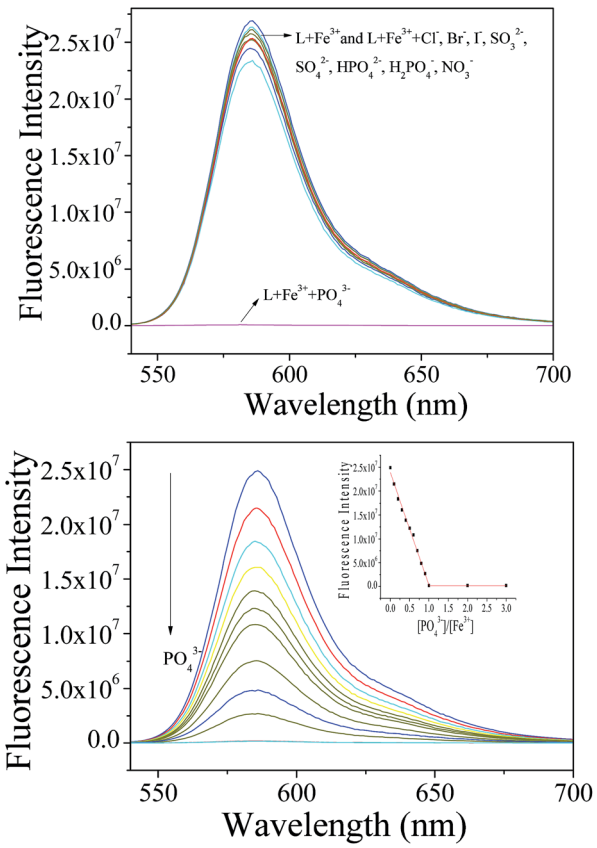


Fig. 7 (a) Fluorescence spectra obtained for L (10 μM) in the presence of $Fe^{3+}$ (80 μM) in $CH_3CN$–Tris (1/1, v/v) 10 min after the addition of various anions (80 μM each), $\lambda_{ex}$ = 520 nm. (b) Fluorescence emission spectra and (inset) variation of fluorescence intensity recorded for L (10 μM) with 8 equiv. $Fe^{3+}$ ions upon gradual addition of $PO_4^{3-}$ (0–30 equiv. for $Fe^{3+}$) in $CH_3CN$–Tris (1/1, v/v). The spectra were obtained 10 min after $PO_4^{3-}$ addition ($\lambda_{ex}$ = 520 nm, $\lambda_{em}$ = 586 nm).

## Conclusions

In summary, we report the synthesis and characterization of a new probe for the cascade fluorogenic detection of trivalent ions and phosphate ions. The probe L showed excellent "OFF–ON" fluorescence signals with high sensitivity and selectivity in the presence of trivalent ions, whereas it remained silent in the presence of monovalent and divalent cations such as $Na^+$, $K^+$, $Mg^{2+}$, $Cu^{2+}$, $Hg^{2+}$, $Cd^{2+}$, $Fe^{2+}$, $Pb^{2+}$, $Zn^{2+}$, $Mn^{2+}$, $Ca^{2+}$. A successive "ON–OFF" fluorescence switching was then observed in the presence of $PO_4^{3-}$ in $CH_3CN$–Tris-buffer (1/1, v/v) media.

## Acknowledgements

The financial support from National Natural Scientific Foundation of China (NNSFC) Project (21204042), China Postdoctoral Science Foundation (2013T60099), National High Technology Research and Development Program of China (863 Program, 2012AA030312), Fundamental Research Project of Shenzhen (JCYJ20120830152316443) and Technology Innovation Program of Shenzhen (CXZZ20130322101824104) are gratefully acknowledged.

## Notes and references

1 Y. Yang, Q. Zhao, W. Feng and F. Li, *Chem. Rev.*, 2012, **113**, 192–270.
2 H. N. Kim, W. X. Ren, J. S. Kim and J. Yoon, *Chem. Soc. Rev.*, 2012, **41**, 3210–3244.
3 L. Yuan, W. Lin, K. Zheng, L. He and W. Huang, *Chem. Soc. Rev.*, 2013, **42**, 622–661.
4 X. Chen, T. Pradhan, F. Wang, J. S. Kim and J. Yoon, *Chem. Rev.*, 2011, **112**, 1910–1956.
5 X. Wan, S. Yao, H. Liu and Y. Yao, *J. Mater. Chem. A*, 2013, **1**, 10505–10512.
6 J.-T. Hou, B.-Y. Liu, K. Li, K.-K. Yu, M.-B. Wu and X.-Q. Yu, *Talanta*, 2013, **116**, 434–440.
7 Y. Lu, S. Huang, Y. Liu, S. He, L. Zhao and X. Zeng, *Org. Lett.*, 2011, **13**, 5274–5277.
8 A. Sahana, A. Banerjee, S. Lohar, B. Sarkar, S. K. Mukhopadhyay and D. Das, *Inorg. Chem.*, 2013, **52**, 3627–3633.
9 J. Mao, L. Wang, W. Dou, X. Tang, Y. Yan and W. Liu, *Org. Lett.*, 2007, **9**, 4567–4570.
10 S. H. Kim, H. S. Choi, J. Kim, S. J. Lee, D. T. Quang and J. S. Kim, *Org. Lett.*, 2009, **12**, 560–563.
11 S. K. Sahoo, D. Sharma, R. K. Bera, G. Crisponi and J. F. Callan, *Chem. Soc. Rev.*, 2012, **41**, 7195–7227.
12 K. Huang, H. Yang, Z. Zhou, M. Yu, F. Li, X. Gao, T. Yi and C. Huang, *Org. Lett.*, 2008, **10**, 2557–2560.
13 D. Maity and T. Govindaraju, *Inorg. Chem.*, 2010, **49**, 7229–7231.
14 W. Lin, L. Yuan, J. Feng and X. Cao, *Eur. J. Org. Chem.*, 2008, **2008**, 2689–2692.
15 S. Goswami, A. Manna, S. Paul, K. Aich, A. K. Das and S. Chakraborty, *Dalton Trans.*, 2013, **42**, 8078–8085.
16 P. Calvo, J. L. Barrio-Manso, F. C. García, J. L. Pablos, T. Torroba and J. M. García, *Polym. Chem.*, 2013, **4**, 4256–4264.
17 J. Mao, Q. He and W. Liu, *Talanta*, 2010, **80**, 2093–2098.
18 L. Yang, W. Yang, D. Xu, Z. Zhang and A. Liu, *Dyes Pigm.*, 2013, **97**, 168–174.
19 A. J. Weerasinghe, F. A. Abebe and E. Sinn, *Tetrahedron Lett.*, 2011, **52**, 5648–5651.
20 Y. Li, Z. Csók, P. Szuroczki, L. Kollár, L. Kiss and S. Kunsági-Máté, *Anal. Chim. Acta*, 2013, **799**, 51–56.
21 Z.-C. Liao, Z.-Y. Yang, Y. Li, B.-D. Wang and Q.-X. Zhou, *Dyes Pigm.*, 2013, **97**, 124–128.
22 M. Yu, R. Yuan, C. Shi, W. Zhou, L. Wei and Z. Li, *Dyes Pigm.*, 2013, **99**, 887–894.
23 P. A. Gale, N. Busschaert, C. J. Haynes, L. E. Karagiannidis and I. L. Kirby, *Chem. Soc. Rev.*, 2014, **43**, 205–241.
24 P. Saluja, N. Kaur, N. Singh and D. O. Jang, *Tetrahedron Lett.*, 2012, **53**, 3292–3295.
25 P. Saluja, N. Kaur, N. Singh and D. O. Jang, *Tetrahedron Lett.*, 2012, **53**, 3292–3295.
26 S. B. Maity and P. K. Bharadwaj, *Inorg. Chem.*, 2013, **52**, 1161–1163.
27 Y. Sun and S. Wang, *Inorg. Chem.*, 2010, **49**, 4394–4404.
28 S. He, S. T. Iacono, S. M. Budy, A. E. Dennis, D. W. Smith and R. C. Smith, *J. Mater. Chem.*, 2008, **18**, 1970–1976.
29 G. V. Zyryanov, M. A. Palacios and P. Anzenbacher, *Angew. Chem., Int. Ed.*, 2007, **46**, 7849–7852.
30 X. Peng, Y. Xu, S. Sun, Y. Wu and J. Fan, *Org. Biomol. Chem.*, 2007, **5**, 226–228.
31 S. Khatua, S. H. Choi, J. Lee, K. Kim, Y. Do and D. G. Churchill, *Inorg. Chem.*, 2009, **48**, 2993–2999.
32 V. Dujols, F. Ford and A. W. Czarnik, *J. Am. Chem. Soc.*, 1997, **119**, 7386–7387.
33 Z. Hu, C. Lin, X. Wang, L. Ding, C. Cui, S. Liu and H. Lu, *Chem. Commun.*, 2010, **46**, 3765.
34 E. M. Nolan and S. J. Lippard, *Chem. Rev.*, 2008, **108**, 3443–3480.
35 X. Fang, S. Zhang, G. Zhao, W. Zhang, J. Xu, A. Ren, C. Wu and W. Yang, *Dyes Pigm.*, 2014, **101**, 58–66.
36 H.-S. Lv, S.-Y. Huang, B.-X. Zhao and J.-Y. Miao, *Anal. Chim. Acta*, 2013, **788**, 177–182.
37 H. Wang, F. He, R. Yan, X. Wang, X. Zhu and L. Li, *ACS Appl. Mater. Interfaces*, 2013, **5**, 8254–8259.
38 C. R. Lohani, J.-M. Kim, S.-Y. Chung, J. Yoon and K.-H. Lee, *Analyst*, 2010, **135**, 2079–2084.
39 G. Zhang, B. Lu and Y. Wen, *Sens. Actuators, B*, 2012, **171**, 786–794.
40 Y. Zhou, J. Zhang, L. Zhang, Q. Zhang, T. Ma and J. Niu, *Dyes Pigm.*, 2013, **97**(1), 148–154.
41 S. Goswami, K. Aich, A. K. Das, A. Manna and S. Das, *RSC Adv.*, 2013, **3**(7), 2412–2416.
42 A. Barba-Bon, A. M. Costero, S. Gil, M. Parra, J. Soto, R. Martínez-Máñez and F. Sancenón, *Chem. Commun.*, 2012, **48**(24), 3000–3002.
43 A. KumaráDas and T. KumaráMondal, *Chem. Commun.*, 2013, **49**(91), 10739–10741.

44 A. K. Mandal, M. Suresh, P. Das, E. Suresh, M. Baidya, S. K. Ghosh and A. Das, *Org. Lett.*, 2012, **14**(12), 2980–2983.
45 A. Liu, L. Yang, Z. Zhang, Z. Zhang and D. Xu, *Dyes Pigm.*, 2013, **99**(2), 472–479.
46 K. Tiwari, M. Mishra and V. P. Singh, *RSC Adv.*, 2013, **3**(30), 12124–12132.
47 H. Liu, X. Wan, T. Liu, Y. Li and Y. Yao, *Sens. Actuators, B*, 2014, **200**, 191–197.